STATIC STABILITY OF A THREE-DIMENSIONAL SPACE TRUSS

John F. Shaker
NASA Lewis Research Center
Cleveland, Ohio

Abstract - Space Station requirements for power have resulted in a need for photovoltaic solar arrays possessing large blanket surface area. However, due to the limited Shuttle payload volume solar array designers have been driven to a deployable concept that by nature is extremely flexible. The principal support for this array system is the **F**olding **A**rticulating **S**quare **T**russ **M**ast (FASTMast). In order to accommodate service loads the FASTMast is expected to exhibit nonlinear behavior which could possibly result in structural instability. Presented herein are the results of the Lewis Research Center test and analysis efforts performed in an effort to characterize the FASTMast structural behavior in terms of stability. Results include those obtained from recent nonlinear testing and analysis involving a 1/10 segment of the FASTMast flight article. Implications of these results as they relate to expected behavior of the flight unit will also be discussed.

INTRODUCTION

In order to characterize complex structures with any degree of accuracy it is necessary to update finite element (FE) models using appropriate test data. In general the approach involves a two-fold process whereby a structural model is optimized utilizing FE modeling methods and response data obtained from characterization tests. Test data is used to either validate or modify original assumptions used when creating an idealized computational model. In many cases the finite element method (FEM) is limited in terms of representation of structural behavior that deviates from linear-elastic response regime. In addition to improving the accuracy of response predictions this approach also reduces the cost of structural characterization by minimizing the amount of required testing. Once a FE model has been test verified it can be exercised repeatedly until all desired response information has been obtained. Although computational costs can also be expensive they are generally much less than those associated with structural testing. Due the complex nature of the FASTMast structure and the limited resources available, this approach was taken to identify the load states at which the strucutre becomes unstable. The objective of this initial study was to create a FE model of the FASTMast structure and attempt to correlate response states to those obtained to from a static structural test involving various applied loads. Utilizing the test results as a guide, appropriate model parameters were updated and analyses repeated until agreement between test data and FE results was achieved. It is clear from the results that this methodology can be used to effectively treat the stability characterization of this structure.

In order to deploy large flexible space structures it is necessary to develop support systems that are strong and lightweight. The most recent example of this aerospace design need is vividly evident in the Space Station solar array assembly. In order to accommodate both weight limitations and strength performance criteria, ABLE Engineering has developed the (FASTMast) support structure. The FASTMast is a space truss/mechanism hybrid that can provide system support while adhering to stringent packaging demands. However, due to its slender nature and anticipated loading, stability characterization is a critical part of the design process. Furthermore, the dire consequences surely to result from a catastrophic instability quickly provide the motivation for careful examination of this problem.

Shown in figure (1) is the solar array assembly of the Space Station Freedom. Once fully deployed the FASTMast strucutre will provide structural support for the solar array system. A unique feature of this

structure is that the system responds linearly within a certain range of operating loads and nonlinearly when that range is exceeded. However, this study involves the nonlinear large displacement problem only since it yields the lowest load levels leading to a state of instability. A complete examination of the FASTMast stability problem is given in reference (1).

HARDWARE DESCRIPTION

Due to electric power demands of the Space Station user community it was necessary to provide solar array assemblies much larger than normally used for space flight. Limited by the modest payload volume of the Space Shuttle, designers were immediately driven to a deployable concept that could accommodate packaging and weight constraints. In order to support the solar array blanket it was necessary to design a support structure that possessed the strength characteristics of a space truss with the mechanistic features of a deployable structure. The answer to this problem was provided by ABLE Engineering with the FASTMast deployable mast assembly.

The FASTMast structure is comprised of thirty-two interconnected **bays** of mast. A complete flight unit will stand approximately 104 feet in length and supports two solar arrays which are a total of 40 feet in width. The total weight of this structure including the mast canister and blanket boxes required for launch support is 2500 pounds. It is designed to provide 18KW of electrical power to the Space Station user community. Shown in figure (2) is a detailed description of the primary components that make up a single bay of mast structure. The longhorns are the primary axial and moment load carrying elements of the structure. In order to provide additional buckling resistance the longerons in the lower twenty bays possess a tapered cross-section. The engineering properties of all major structural components are given in tables (1) and (2).

The principal elements providing resistance to shear and torsional loading are the prestrained stainless steel 7X7 wire rope diagonals. In addition to the shear resistance provided by this structural member it also provides flexibility that is required of a deployable structure. The current design preload level in this element is 31 pounds. Supplying the load required for diagonal prestrain is the fiberglass flex batten. In order to create the necessary force the flex batten is installed in a post-buckled state. The buckled shape of this element is clearly visible from the top view of the mast given in figure (3). A direct analogy to this design concept is the energy transmitted to an string from a buckled bow.

In addition to reacting the preload of the flex batten, the elbow joints provide a pivot point required for mast stowage and deployment. Therefore, it was necessary to design this joint with a dual-function end fixity. In order to facilitate the folding action of the mast the elbow joints act as a hinge in the direction of rotation required for stowage. Shown in figure (4) is the manner in which the elbow joint, flex batten, and diagonal elements are connected to the mast. Figure (5) shows the diagonal to longeron connection which is made with a bracket and two 4-40 socket-head cap screws. Also given in this drawing is a clear view of the folding direction of the longeron/flex batten interface. The pinned and hinged boundary conditions at this joint are associated with the Euler buckling and large displacement failure modes respectively. The pinned condition exists at this interface when hinge action is not taking place.

At the top and bottom of each bay of FASTMast are the rigid battens and the corner fittings. These structural elements provide a pivot point for the longeron at the top of the bay and anchor the rigid battens to the space lattice. Rigid battens provide shear and torsion load resistance by restraining corner fitting motion. The taper feature of the rigid batten was incorporated in order to reduce weight and increase strength of the element. The diagonals are mounted at the top of the bay in a manner similar to that described above.

Although the individual elements of the FASTMast structure do not possess large strength capability the integrated unit appears capable of withstanding service loads. However, in order to achieve the required strength to weight ratio this type of structure presents an obvious stability problem. Further complicating this problem is the fact that there exists both a local and global instability modes each influenced by deformed mast geometries and applied loading conditions.

NONLINEAR FAILURE MODE IDENTIFICATION

The allowable load of a structure is a function of its design and the anticipated failure mode. Determination of allowable load requires a clear understanding of structural behavior during loading events and identifying the appropriate mode of failure. Once these two goals have been achieved a valid analytical model can be constructed and the allowable load of the structure can be determined.

The FASTMast will be subjected to a combined state of moment (M), axial (A), shear (V), and torsion (T) load as graphically depicted in figure (6). From a simple static assessment of the mast it is clear that applied shear torsion loads are reacted in essentially the same manner. This figure merely attempts to present a simplified representation of all possible applied loads at a system level. Nonlinear behavior of the FASTMast structure is due principally to the changing stiffness state of the structure that results from slack diagonals. As was previously stated shear and torsion loading is reacted internally by the diagonals and battens. An attempt to illustrate mast reaction to shear load is given in figures (7) and (8). Shown in this figure is the action of the flex batten and diagonals due to the action of preload P and shear load V. The shear and torsional stiffness of the mast is a result of the post-buckled flex batten force P inducing a tensile preload in the wire diagonals. The load state in figure (7) is a result of only preload P while the manner in which the mast will react shear load V is illustrated in figure (8). The sum of figures (7) and (8) represents the combined action of V and P. It is assumed that each diagonal is prestrained to the same level while resisting shear load equally. The flex batten reaction to the shear load is zero because it is in a post-buckled state and cannot take additional load. Although figure (8) indicates that a set of diagonals would be in "compression", physically this equates to a reduction of the force P supplied by the flex batten. The limiting state is reached when the load in the "compressed" diagonal becomes zero (slack condition), at which time the flex batten begins to pick up additional compressive load and the mast begins to move into a fold-up mode required for mast retraction (figure 9). The applied shear level at which unwanted mast stowage occurs is that required to overcome the preload in the wire diagonals. A shear load of this magnitude is much lower than that required for material yield in either the diagonal or flex batten. Therefore the principal failure mode for applied loads involving shear and torsion is structural instability.

Based upon the preliminary failure mode assessment above it is clear that an evaluation of FASTMast stability should be undertaken. From initial instability considerations it was determined that the deformed state during instability would be either a local or global deformation as given in figure (10). A global or system failure event would correspond to the fold-up mode that results from excessive shear/torsion and axial load . Fold-up in this instance is defined to be mast action which occurs during a solar array restowing event. The instability event involving mast fold-up is mechanistic in nature and is due to the nature of the FASTMast design which involves both truss and mechanism elements. Furthermore, due to mast stiffness changes which occur during large deflections of the elbow joint, this form of instability is nonlinear in nature. On the other hand, the local failure mode involves the classic general instability of a pinned-pinned column subjected to an axial load which would occur during excessive moment and axial loading on the mast. The local instability event involves Euler buckling of a single longeron as is shown in figures (10) and (11) and is a linear response event. The principal difference between these two failure modes is that the system event is kinematic in nature. Also, the local event does not involve nonlinear behavior indicative of the system type failure mode.

APPROACH

After considering both problem physics and resource limitations it was decided that a one-tenth segment of FASTMast structure could be used to meet study objectives. This one-tenth model of the flight hardware is referred to as the *3-bay* FASTMast unit. Furthermore, due to the symmetric nature of the structural load paths extending the test verified 3-bay theory to the 32-bay flight unit configuration was considered plausible. Based upon these initial assumptions parallel test and analysis efforts involving FASTMast nonlinear stability assessments were design and executed.

THREE-DIMENSIONAL NONLINEAR LARGE DISPLACEMENT ANALYSIS

The source of nonlinearity in this case is due to the changing system stiffness as the structure experiences large deflections. This particular large displacement problem includes the effects of large translations and rotations while strains remain small. However, in order to accurately predict nonlinear behavior it is extremely important the FE model closely match the nonlinear elements of the hardware. Therefore, accurate modeling of the flex battens, wire diagonals, and mast joints was deemed critical for generation of accurate and valid data.

The model used for this analysis was created with the ANSYS finite element code. ANSYS was selected due to its proven nonlinear capabilities. The entire model consisted of 312 elements, 225 nodes, and an estimated 1330 degrees of freedom. Shown in figure (12) is the undeformed preloaded ANSYS model. In order to define the entire model five element types and ten real constant sets were required. All mast structural properties were based on the most-up-to-date information available.

The longerons were modeled using three-dimensional tapered beams thus reflecting the design of the lower twenty bays of the flight unit. Each rigid batten frame required three-dimensional truss elements to model the batten tube and three-dimensional tapered beams to model the corner fittings. The wire diagonals were represented by two-dimensional tension only spar elements which included an initial prestrain equal to that prescribed by the required tensile preload. Finally, the fiberglass flex battens were also represented by three-dimensional beam elements.

In order to represent joint flexibilities at the elbow and corner fittings hinge elements were introduced to these parts of the structure. The ANSYS hinge joint provides translational and rotational stiffness in all six degrees of freedom at the point of application. At each elbow joint there are four hinge elements and at each corner fitting there are two. A hinge element consists of a coincident node pair that are connected in all but one rotational degree of freedom. Shown in figure (13) is an example of an elbow joint modeled using hinge elements. In this example the coincident node pairs are (5,45), (5,35), (5,25), and (5,15). At each longeron end there is a hinge that allows for ninety-degree rotation plus a 0.6 degree back rotation required to model stopping action of the deploying mast. After engaging the stop the hinge is no longer free to rotate and instead behaves as a torsional spring with a rotational stiffness of 1×10^6 in-lb/rad. The hinges on flex batten ends do not have rotational limits and possess very high translational stiffnesses. An identical connection process is carried out at the corner fittings without the inclusion of the flex batten.

The ability to identify instability points during a geometric nonlinear large displacement analysis is not straightforward. Unlike linear static analyses, the structure is loaded incrementally and the equations of motion are solved in a piecewise linear manner over subintervals of the response regime. Over each loading increment the equations of equilibrium are solved iteratively until the solution converges within some specified tolerance ban. During this analysis both force and moment convergence criteria were

used to evaluate the adequacy of the solution before proceeding to the next load step. Solution iterations continue until either convergence is achieved or the analysis is terminated by user request. Upon successfully satisfying the equations of equilibrium the stiffness matrix is updated and the analysis moves to the next interval of applied load. This process is repeated over the entire range of applied load. The fact that the solution is derived in a piecewise manner introduces the first analytical difficulty which involves bypassing the point of instability due to an interval selection that is too broad. This situation can occur for instabilities such as "snap through" buckling. Furthermore, even if the proper interval has been identified there still remains the question of at which point in the interval instability will actually occur. For example, if an instability occurred between ten and twenty pounds the failure load level possibilities include eleven, twelve, ... , and twenty pounds. The only explicit conclusion presented by code output is that a failure occurred somewhere between the end points of the applied load interval. Also, identification of instability points from output data can be accomplished by identifying radical changes in output values at some predefined characteristic point. In this case large displacements at the top of the mast due to a load of smaller or equal magnitude than the preceding step was taken to infer a point of instability. An analytical consequence of such an event may result in a set of equilibrium equations that prove to be nonconvergent. This type of nonconvergence is due to the fact that the structure has undergone a shape change that will not satisfy conditions of equilibrium. However, convergence problems may also result from modeling errors that have no relationship to a possible state of instability. Therefore, prior to reporting large displacements and nonconvergent behavior as indications of instability points structural response must be judged appropriate. The analyst must ensure that the FE model is accurately representing nonlinear behavior and results reflect problem physics. In general this is accomplished by utilizing engineering insight and structural test data during the data reduction process.

The focus for this particular model correlation activity resided with the hinge elements. At each node involving a hinge element there are six degrees of freedom five of which must be assigned stiffness values. The sixth degree of freedom is that of the primary hinge rotational direction which for this study was taken to be frictionless. Of the remaining five degrees of freedom only the lateral and axial stiffnesses were updated with the aid of results from stiffness testing. Stiffness values were obtained by performing a longeron axial load test and a system level lateral load test. The model hinge stiffness parameters were then updated and a nonlinear analysis of the configuration given in figure (14) was performed and compared to test results. The remaining translational and rotational hinge stiffnesses were assumed to be either zero or very large and that fact is reflected in the FE model.

STIFFNESS TESTING

In order to generate the required stiffness values an axial stiffness of the longeron/elbow joint was performed in addition to a tip shear stiffness test. The test configurations are shown in figures (16) and (17). Stiffness testing was performed by agents of the Engineering Directorate of Lewis Research Center (LeRC) and details are available in references (2) and (3).

The first model update was performed using stiffness data from an axial stiffness test which was configured as shown in figure (17). The test specimen consisted of an elbow fitting and two square longerons and was loaded in a series of ten load steps to final level of 4200 lbs. As the load level reached 3000 lbs nominal yielding of the strucutre had occurred. Yielding of the specimen increased dramatically over the range of 3000 to 4500 lbs at which point the test was terminated. Linear behavior was observed throughout the 2400 lb load case with yield occurring at approximately 2500 lbs. A linear fit of the test data resulted in the load/displacement curve with a slope of 4.3×10^5 lb/in which represents the axial stiffness of the hinge.

Updating of the lateral elbow joint stiffness was made using results from the 3-bay lateral loads test. The system level lateral load test was performed in a manner that allowed for sequential loading of the truss

strucutre until a limit value was achieved. A lateral load of 120 lbs was applied to the structure in a stepped fashion and the displacements were recorded at locations given in figure (15). The nonlinear behavior of the FASTMast is clearly evident in figure (18) which gives the deflection of the mast top as a function of lateral load. The system response becomes nonlinear as the applied load reaches a level of 83 pounds. This bilinear behavior is due to the fact that the diagonal tension has been reduced to zero and the flex battens begin to react the applied load. The mast stiffness up to the 83 lb inflection point is approximately 332 lbs/in and decreases to 28 lbs/in at the onset of nonlinear behavior. In order to achieve model correlation an attempt was made to match analytically the test results given in figure (18) by adjusting the lateral stiffness of the elbow joint.

RESULTS AND DISCUSSION

The results of the structural testing and nonlinear large displacement analyses are given graphically in figure (19). In this figure the lateral displacement of the 3-bay FASTMast is plotted as a function of lateral load. The top curve represents the system response identified during the 3-bay lateral load test and the remaining curves show results from the nonlinear analyses. A total of three FE model updates were made in support of this study. For each analysis the lateral load was equal to 120 lbs applied in twelve equal load steps of 10 lbs. In all three cases there was no evidence of a structural instability. As a starting point all hinge stiffnesseses were modeled as rigid connections. As expected this resulted in a mast stiffness much higher than that observed in test. System performance with rigid hinge connections is shown in the lower-most in curve of figure (19). The results indicate a system stiffness of 796 lb/in in the linear regime, and 34 lb/in during nonlinear response. The first update of the model consisted of modifying the axial stiffness of the hinge joint to a value 4.3×10^5 lb/in. This change resulted in a linear system stiffness of 667 lb/in, and a nonlinear stiffness of 33 lb/in. Finally, the lateral stiffness of the hinge elements was updated to a value of 400 lb/in. This value was determined from a recent hinge joint test of the 3-bay unit. From figure (19) it is clear that this change results in a dramatic increase in system flexibility. The slope of the curve depicting these results indicates a linear stiffness of 515 lb/in and nonlinear stiffness of 24 lb/in. Therefore, the final updated model possess a 54% error in linear stiffness and -14% error in nonlinear stiffness. For this study a negative error rate implies excessive flexibility exists in the model as compared to test results. Although model results improved over the updating process more work will be required to obtain a better model correlation.

A second interesting result shown in figure (19) is that the onset of nonlinear behavior given by analysis differs from that found during testing. The test results indicate that nonlinear behavior begins at an applied lateral load level of 84 lbs while the analytical level is approximately 100 lbs. This discrepancy could be the result of several possible test and/or model anomalies which may include: (1) variation in anticipated test article diagonal preload, (2) model hinge stiffness inaccuracies, (3) excessively stiff model of the rigid batten, and (4) inaccurate value of Young's modulus for the flex batten. Each of these items will be examined during the remainder of the model correlation effort in order to identify the source of this discrepancy.

In terms of structural performance it is clear that resistance to applied loads will decrease dramatically when the FASTMast enters a nonlinear response regime. Furthermore, if the predominant failure mode is instability collapse will be sudden and catastrophic. Therefore, it would prudent to restrict mast operations to the linear regime.

SUMMARY

The results presented herein indicate that FE model updating techniques can be successively employed when analyzing large flexible structures. However, reliable updates to complex elements such as rotating hinges and preloaded elements can only be achieved utilizing test data and sound updating procedures. Once the FE model has been test verified, characterization of system responses can be achieved with greater levels of accuracy and validity.

REFERENCES

1. Shaker, John F., Static Stability of a Three-Dimensional Space Truss , M.S. Project,Case Western Reserve University, 1994.

2. 3-Bay FASTMast Shear Test and Analysis, Lewis Research Center Engineering Report No. SAB 93-003, April 1993.

3. PV Structural Analysis Space Station Tension Test of FASTMast Elbow Joint, Lewis Research Center Engineering Report No. 93-3.

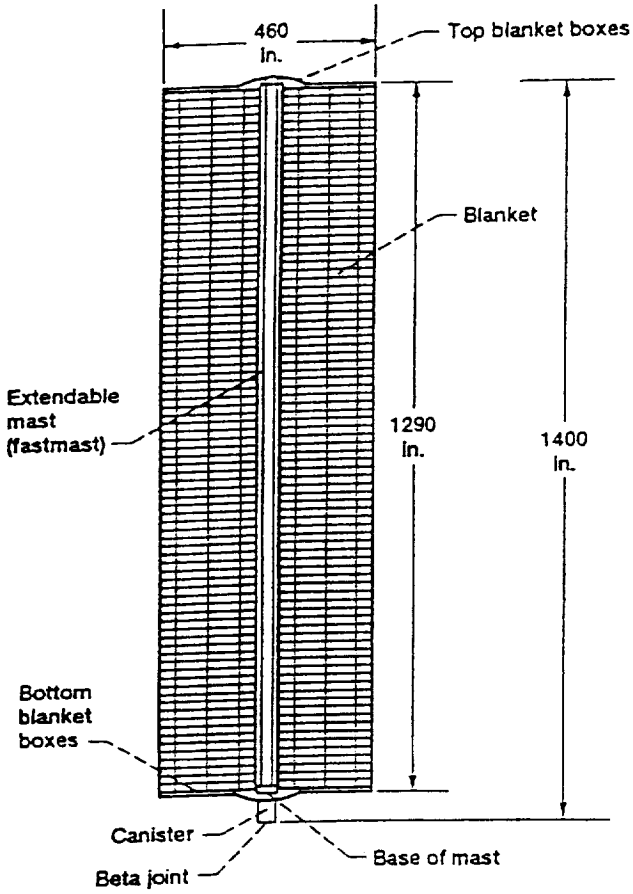

Figure 1 - Space Station Solar Array

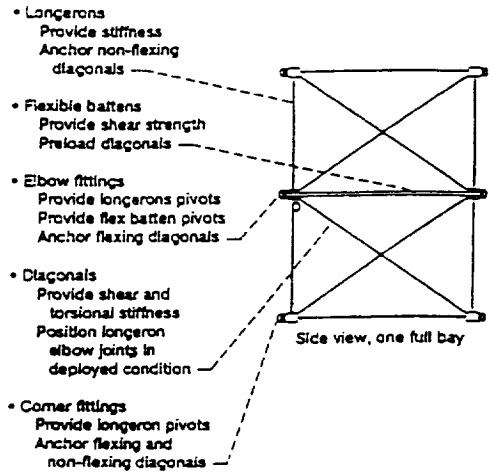

Figure 2 - FASTMast Structure

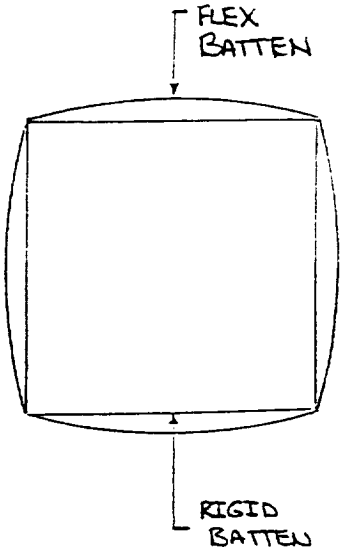

Figure 3 - FASTMast (top view)

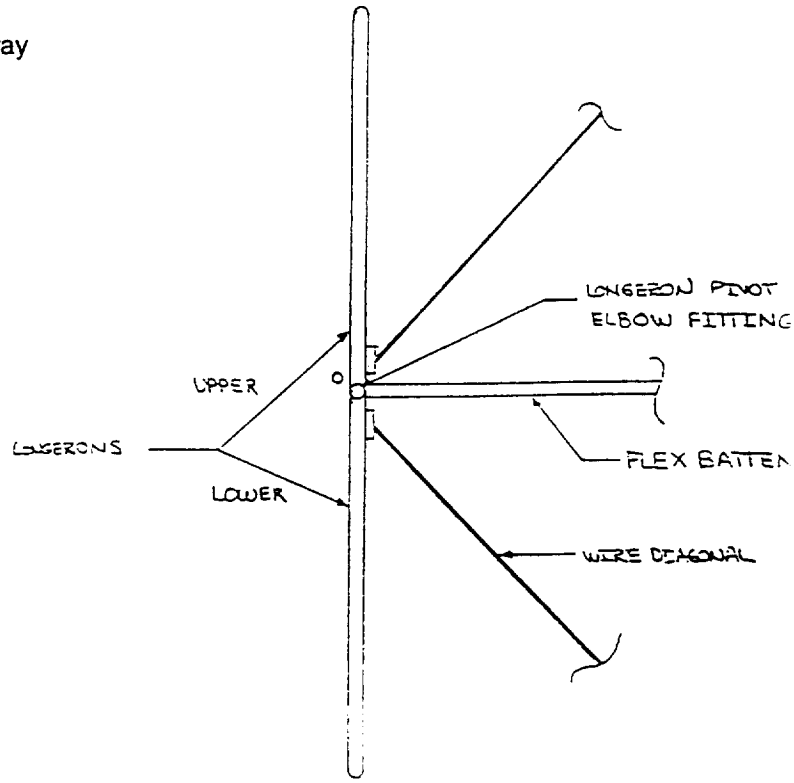

Figure 4 - Flex Batten / Longeron Interface

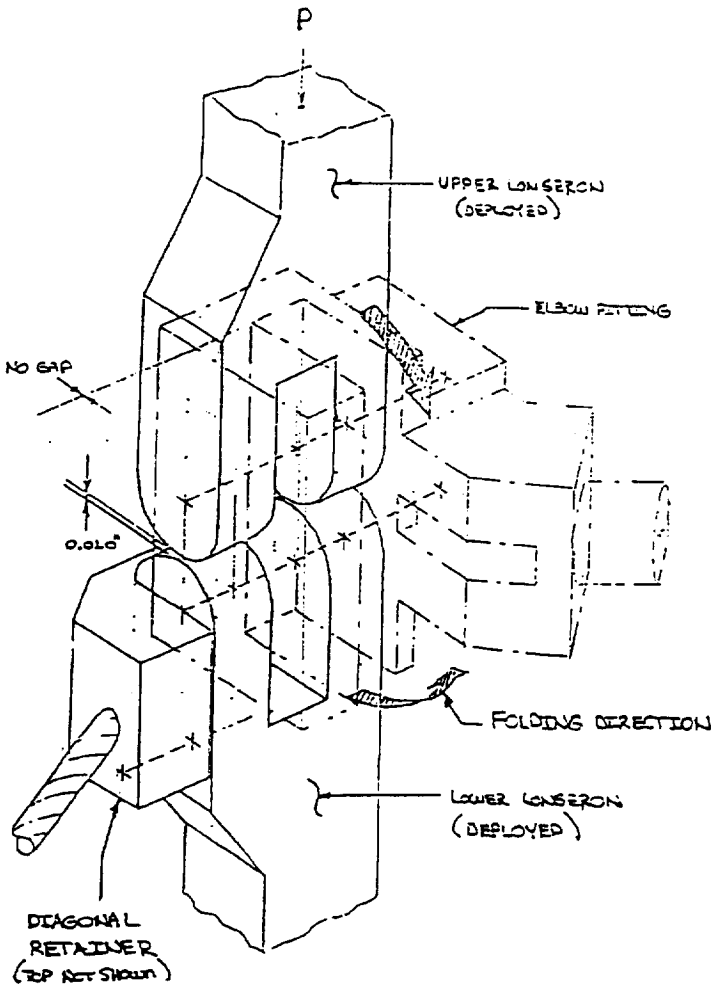

Figure 5 - Elbow Fitting Longeron Interface

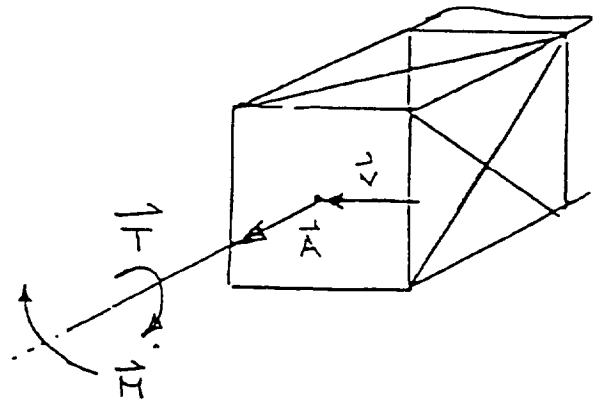

Figure 6 - FASTMast System Loading

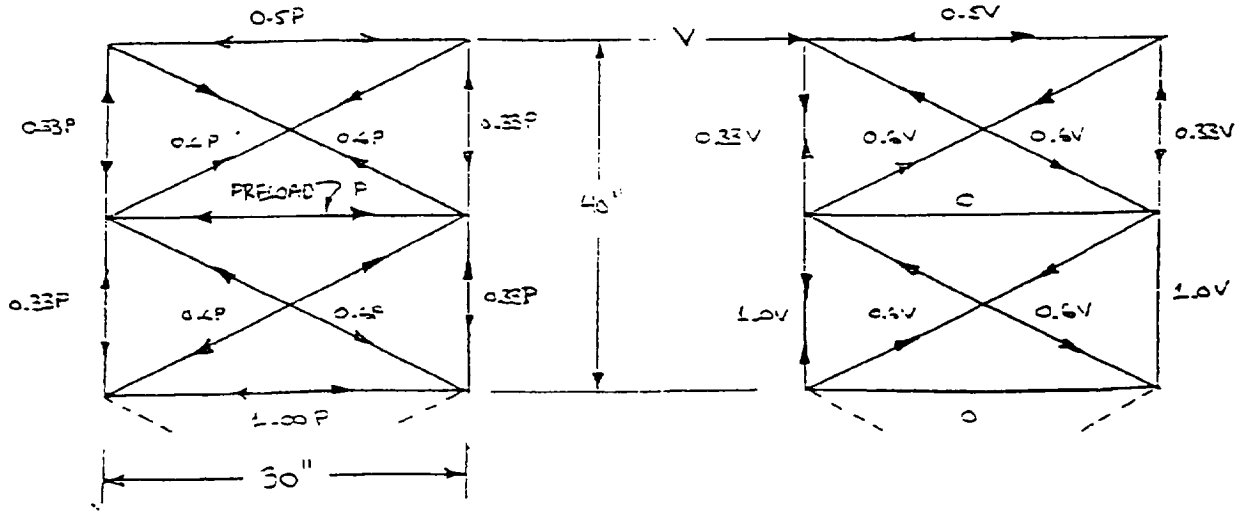

Figure 7 - FASTMast Preload Reactions

Figure 8 - FASTMast Shear Load Reaction

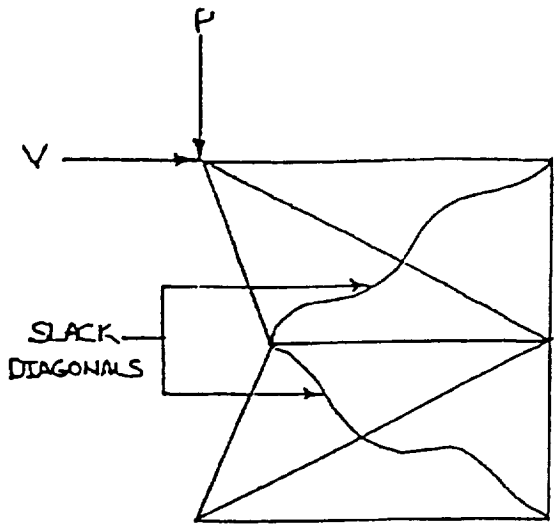

Figure 9 - FASTMast Fold-up Action

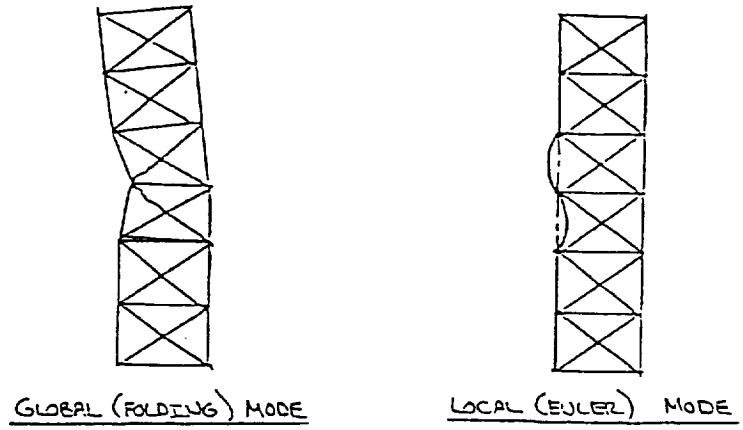

Figure 10 - FASTMast Failure Modes

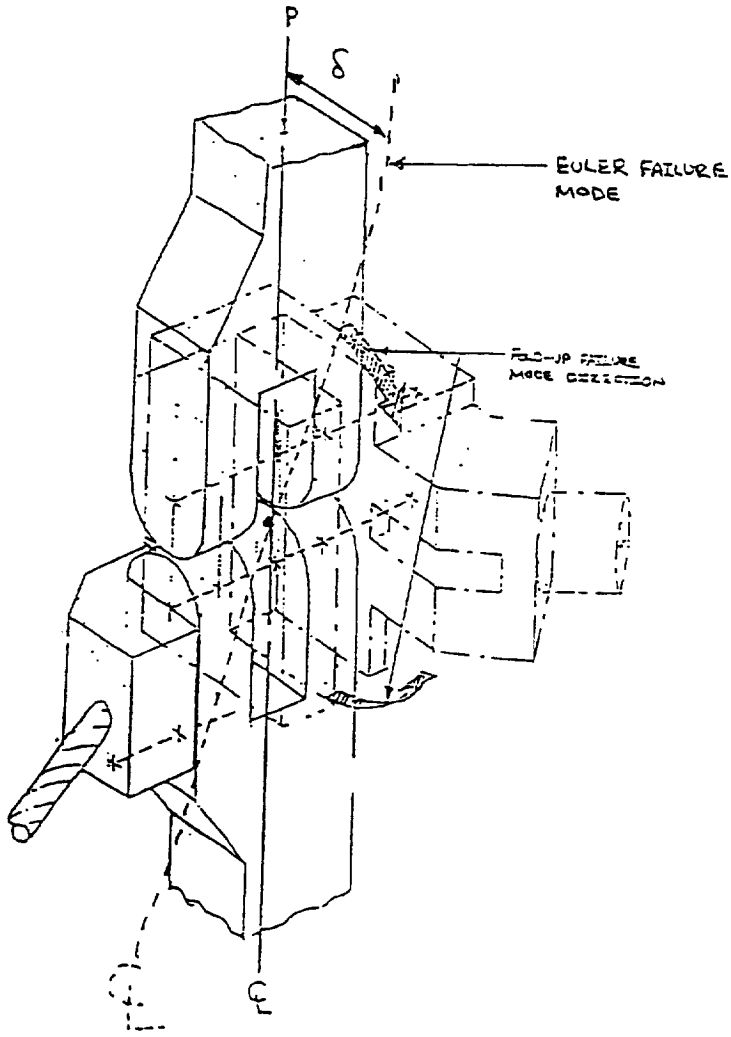

Figure 11 - Longeron Motion During Failure Modes

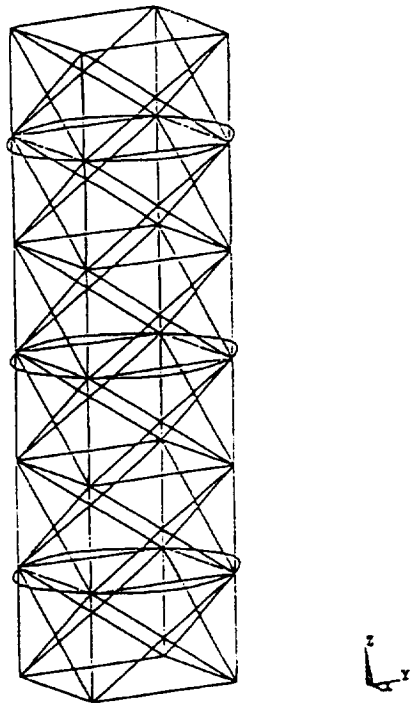

Figure 12 - FASTMast Nonlinear Finite Element Model

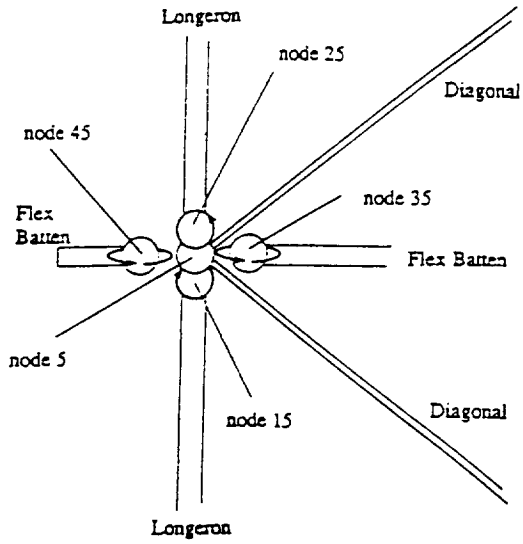

Figure 13 - FASTMast Hinge Joint

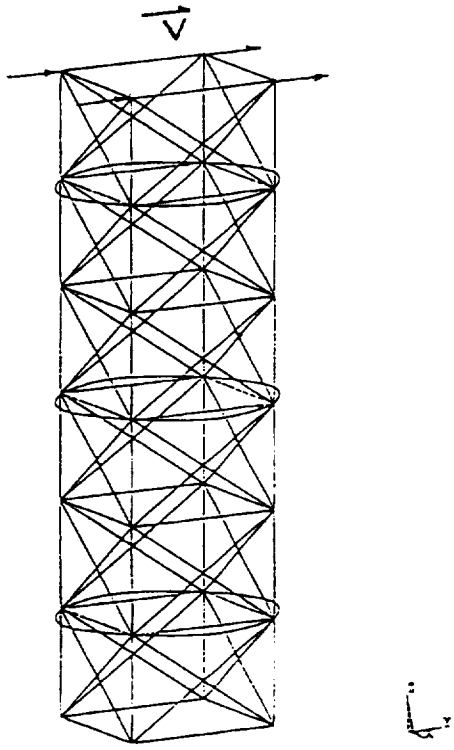

Figure 14 - Nonlinear Finite Element Model Tip Shear Case

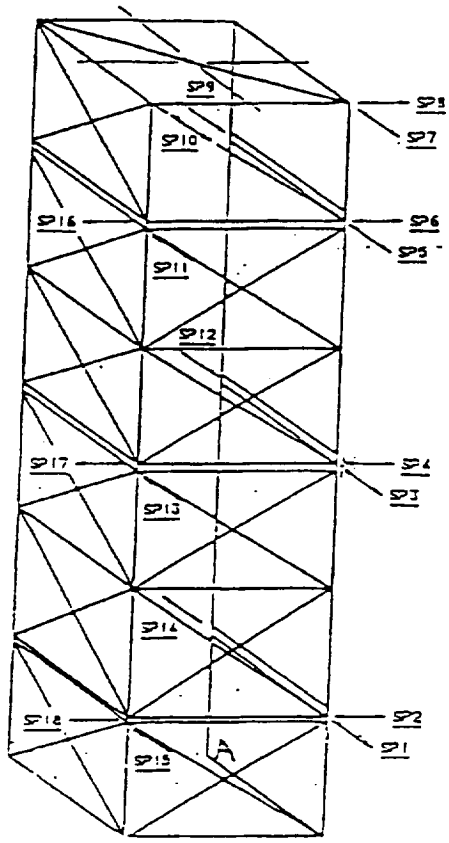

Figure 15 - Displacement Transducer Locations for Tip Shear Test

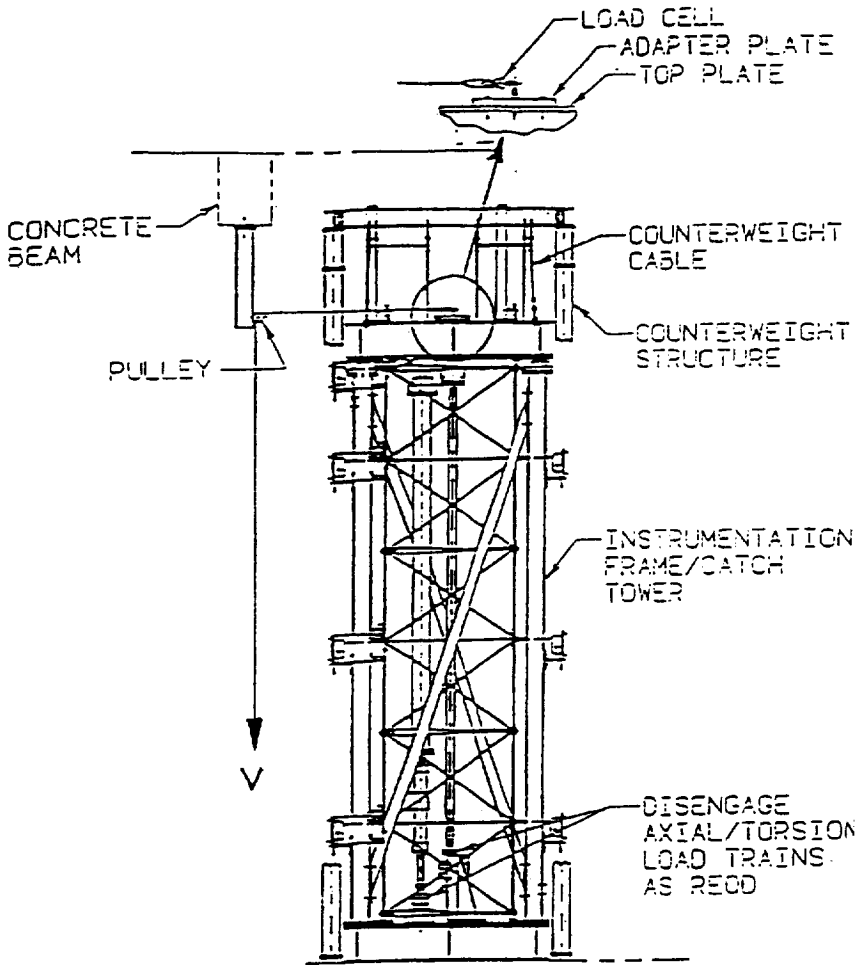

Figure 16 - 3-Bay Tip Shear Test Configuration

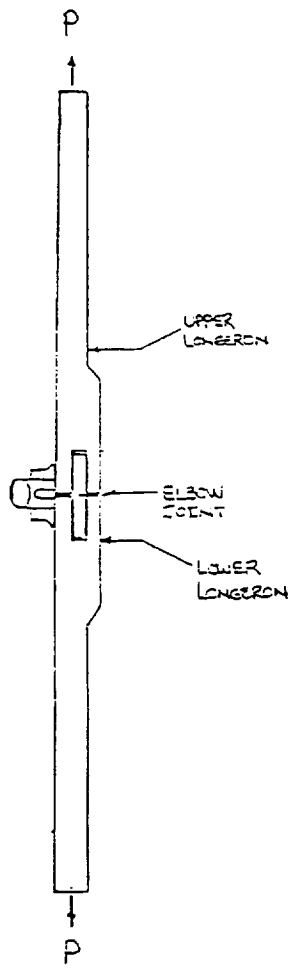

Figure 17 - Longeron Axial Stiffness Test Configuration

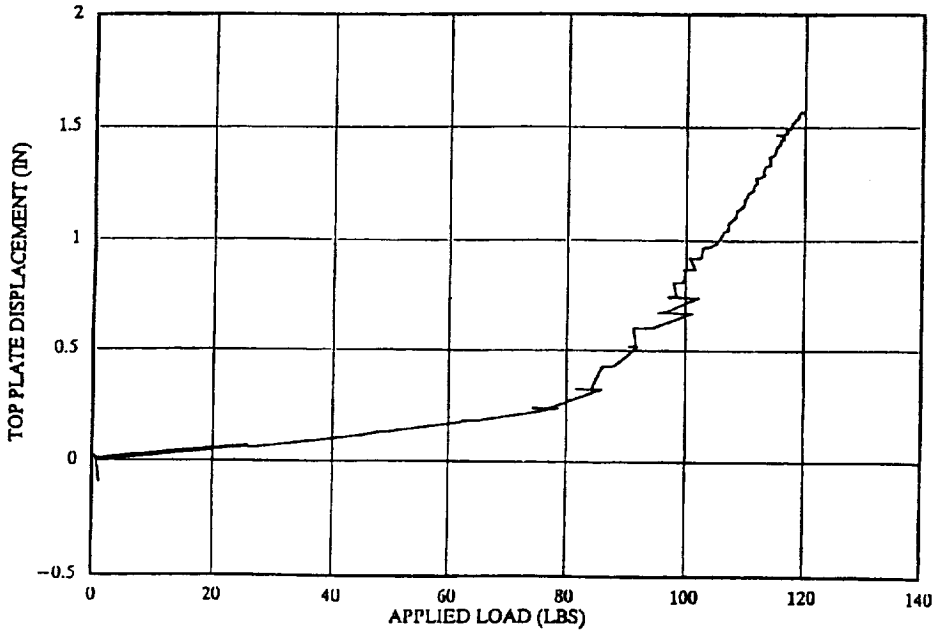

Figure 18 - FASTMast Top Deflection vs. Lateral Load from LeRC Shear Test

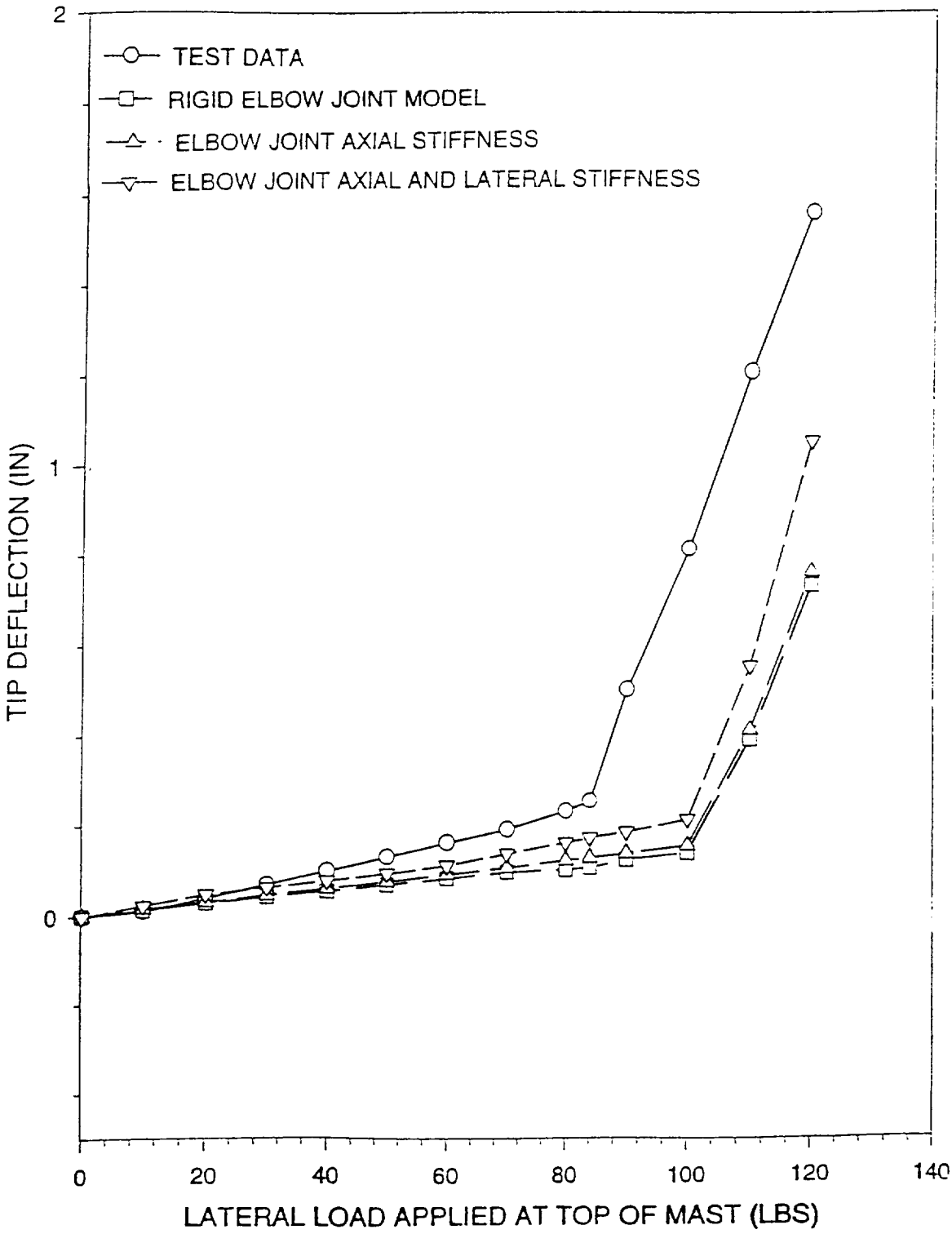

Figure 19 - Test and Analysis Mast Top Deflection vs. Applied Load

Mast Element	Material	Length	Area	Young's Modulus	Movement of Inertia I_{xx}[1]	Movement of Inertia I_{zz}[2]
		IN	IN^2	LB/IN^2	IN^4	IN^4
Tapered Longeron	Aluminum 6061-T6	19.750000	0.348100	10×10^3	0.010100	0.010100
Straight Longeron	Aluminum 6061-T6	19.750000	0.250000	10×10^3	0.005210	0.005210
Rigid Batten	Aluminum 6061-T6	19.300000	0.063900[3] 0.036200[4]	10×10^3	0.017400[3] 0.001440[4]	0.000436[3] 0.000316[4]
Batten Tube	Aluminum 6061-T6	11.200000	0.051110	10×10^3	0.001390	0.001390
Flex Batten	Fiberglass	31.750000	0.103000	8×10^3	0.001210	0.000591
Diagonal	Stainless Steel	36.000000	0.002318	29×10^6	———	———

1. Element y-axis oriented such that with x-axis along length of element right-hand rule is satisfied
2. Element z-axis vertical to cross-section
3. Wide end of tapered section
4. Narrow end of tapered section

Table 1 - Engineering Properties of Principal FASTMast Components

Structural Element	Material	Young's Modulus	Poisson's Ratio	Area	Moment of Inertia	Coefficient of Thermal Expansion
[redacted]		LB/IN^2		IN^2	IN^4	$IN/IN-F^\circ$
Longeron	Al-6061	$10X10^6$	0.33000	0.25000	0.00521	0.0
Flex Batten	Fiberglass	$8X10^3$	0.33000	0.10300	0.00121	$3.0X10^{-7}$
Diagonal	Stainless Steel	$30X10^6$	0.33000	0.00231	N/A	0.0

Table 2 - Properties for Two-Dimensional Nonlinear Planar Truss Study